

COMPUTER SIMULATION OF PRETRANSITIONAL PHENOMENA IN HARD-CORE  
MODELS FOR LIQUID CRYSTALS\*

D. Frenkel  
FOM Institute For Atomic and  
Molecular Physics  
Amsterdam  
The Netherlands

I. Introduction

Van der Waals [1] was the first to suggest that the local structure of dense simple liquids is largely determined by short range repulsive forces. The transformation of this idea from a bold assumption to an almost commonplace statement owes much to the fruitful combination of computer simulations and thermodynamic perturbation theory [2,3,4]. For example, the freezing of atomic liquids can be understood on basis of the fluid-solid transition of hard spheres, first observed by Alder and Wainwright [5]. The liquid-vapor transition does not occur in a pure hard-core system, but can be explained in terms of a weak attractive perturbation added to the repulsive interactions.

It is much less clear to what extent excluded volume effects can help us to understand the thermodynamics and phase transitions of 'complex' liquids, in particular liquid-crystal forming materials. Actually, the question to be addressed is two-fold. Firstly: is it at all possible to explain a particular type of phase transition in a liquid crystal in terms of excluded volume effects alone, or is the presence of other interactions, such as attractive dispersion forces essential? And secondly: even if we find that hard repulsive forces can cause a particular phase transition in a model system, do we have reasons to assume that excluded volume effects are also at the root of such phase transitions in real liquid crystals? To illustrate the latter point, consider the following example: gravitational attraction could cause a liquid-vapor transition in an atomic fluid. Yet, it is clear that gravity is not the explanation for this phenomenon. By analogy, it is conceivable that hard-core repulsions could drive a transition from a nematic to, say, a columnar phase (incidentally, in a simple model system they can), but this does not necessarily imply that repulsive forces are also the dominant factor determining the structure of real discotic liquid crystals.

This paper focuses on the first question which I shall phrase here as: Can hard-

---

\*Part of the material reviewed in this article appeared in the January 1987 issue of Molecular Physics.

core models exhibit the phase transitions and pre-transitional behavior found in liquid crystals? But I stress that a positive answer to this first question only implies that we now have to face the second, i.e.: Do hard-core models contain the essential physics? At present the answer to this second question is open.

Below I shall present the results of recent computer simulations on non-spherical hard-core models. As we shall see, a surprising number of phenomena observed in real liquid-crystal forming materials are reproduced by these simple models. The remainder of this paper is organized as follows: first I shall discuss the effect of molecular shape on the relative stability of crystalline and liquid crystalline phases. Next I shall present some preliminary results on pretransitional fluctuations in nematogens, in particular collective orientational fluctuations. And finally I shall present some recent results on smectic ordering in hard-core model systems.

However, before continuing I should warn the reader. The discussion in this paper is limited to hard-core models. This bias is intentional. I wish to explore the limits of applicability of the hard-particle concept. But I wish to stress that there exists an extensive literature dealing with simulations of other model systems, such as for instance the 'Lebwohl-Lasher' model which has been studied in detail by Luckhurst and collaborators [6] or the simulation of a realistic model for an existing nematogen (see Ref. [7]). Liquid crystals are complex systems, and only by combining the results obtained by experiment, theory and different computer simulation techniques can we hope to increase our understanding of these fascinating materials.

## II. Solid or Nematic?

Most isotropic molecular liquids freeze as the temperature is lowered. But only some form liquid crystals. The obvious question is: what determines whether a molecular liquid forms a liquid crystal before it freezes?

Let us first briefly summarize the essential characteristics of liquid crystals (for details the reader is referred to Ref. [8]). Liquid crystals are partially ordered fluids. The simplest is the nematic phase in which the molecules are translationally disordered but, unlike the isotropic fluid, the molecular orientations are no longer distributed randomly. Rather, the molecular axes tend to align parallel to some, otherwise arbitrary, direction. This alignment axis is usually referred to as the nematic director  $\vec{n}$ . A quantitative measure for the degree of alignment is the nematic order parameter  $S$ . For axially symmetric molecules,  $S$  is defined as  $\langle P_2(\cos\theta) \rangle$ , where  $\theta$  is the angle between the molecular symmetry axis and the nematic director. In the isotropic phase,  $S=0$ . In a perfectly aligned nematic  $S=1$ . The phase transition from isotropic liquid to nematic liquid crystal is weakly first order. By 'weakly first order' I mean that the transition, although first order, is preceded by strong precursor effects as is usually the case in the vicinity of continuous phase transitions. The transition from both the nematic and the isotropic phases to the solid is a normal

first order transition.

All molecules that form nematics are non-spherical, but the converse is not true. In other words, a certain degree of non-sphericity is a necessary, but not a sufficient condition for liquid crystal formation. Several other factors also play a role in determining the relative stability of the nematic phase. For instance, attractive intermolecular interactions due to dispersion forces also tend to favor parallel alignment of the molecules. There are a number of models that attribute the orientational ordering in liquid crystals to the effect of dispersion forces [9,10], including the original mean-field model due to Maier and Saupe. Although these models yield fair estimates for a number of properties of nematic liquid crystals, they cannot be used to explain the stability of the nematic phase with respect to the solid. It is quite conceivable that in some cases dispersion forces would stabilize the solid more than the nematic. Another factor that influences the stability of liquid crystals is the presence of flexible tails (often alkane or alkoxy chains) connected to the 'rigid' core of the nematogen. That flexible chains are indeed important for the stability of liquid crystals follows from the experimental observation that essentially all liquid crystal forming molecules ('mesogens') have them [11]. If the tail is shortened too much, the liquid freezes without ever becoming nematic. Intuitively, the role of flexible tails in stabilizing the liquid crystal with respect to the solid is clear: if a flexible tail has to fit into a crystal lattice, it will lose much of its conformational degrees of freedom with a concomitant loss in entropy. A model that takes into account the effect of the flexible tails on the relative stability of isotropic, nematic and smectic phases was developed by Dowell and Martire [12]. But again, to my knowledge, a quantitative comparison with the solid has not been made.

The question which remains is: which of the factors mentioned above has the most important effect? For someone who is familiar with the theory of simple liquids it is natural to assume that the hard-core repulsions are most important. Of course, the 'natural' assumption is not necessarily the correct one, and the only way to find out is to try. Trying in this case means computer simulation. Still I would like to present some justifications for my assumption that molecular shape effects are of primary importance while dispersion forces and flexibility effects can be considered as 'perturbations'. Onsager [13] has shown that the isotropic-nematic transition can take place in a simple model that considers only the non-spherical excluded volume effects. In contrast, flexible tails alone cannot cause nematic order. Neither can anisotropic dispersion forces. To be more precise: a model which only includes dispersion forces but no hard-core repulsion will collapse. Of course, if one adds a spherical hard-core repulsion, anisotropic dispersion forces can explain the transition to a nematic phase, but in nature a molecule with a spherical hard core will not have anisotropic van der Waals interactions. Hence, in the real world, anisotropy in the dispersion forces implies a non-spherical hard core anyway. Of course, the converse is also true but, at least for sufficiently non-spherical particles, dispersion forces appear relatively

unimportant. In summary, non-spherical hard-core repulsion is the most plausible mechanism to explain the formation of a nematic phase without the help of any of the other factors. It seems reasonable then, to treat hard-core repulsion as the 'primary' effect. One may hope that some kind of the thermodynamic perturbation theory can, at a later stage, take the effect of dispersion and flexibility into account. However, I should stress that at this stage we do not yet have any evidence that such a perturbation scheme will work.

Before we turn to the computer simulation let me briefly sketch what we know from experiment about the relation between molecular shape and the tendency to form liquid crystals [14]. First of all, we know that liquid crystals can consist of both rodlike and platelike molecules. Most rodlike mesogens have length-to-breadth ratios between 3 and 4 (it should be noted, however, that this ratio is a rather fuzzy concept for molecules with flexible tails). What we know at present about disclike mesogens (see e.g. 15) suggests that these molecules are even less spherical. It is not straightforward to tell from experiment how the isotropic-nematic and the nematic-solid transition depend on the shape of the repulsive core of the molecules. The problem is that although a wealth of data on the phase transitions of molecules with different shapes are available, we do not know how to disentangle the effects of molecular shape, dispersion forces and flexible tails.

Next, let us consider what we know from theory and earlier computer simulations. For hard spheres we do know the melting point from the computer simulations of Hoover and Ree [16]. But these simulations do not tell us what will happen to the melting point as the molecular shape changes from spherical to rodlike or platelike. The Onsager theory [13] predicts that thin spherocylinders with length  $L$  and diameter  $D$  undergo a transition from the isotropic to the nematic phase at a density of order  $1/(L^2D)$ . At this density the fraction of the volume occupied by the spherocylinders is still vanishingly small (order  $D/L$ ). The same holds for infinitely thin hard platelets [17]. For neither of these model systems do we know the melting point.

### III. Computer Simulations of Nematogens

#### III.1 General Remarks

To fill this gap in our knowledge about the phase behavior of non-spherical hard-core molecules, we performed Monte Carlo simulations on a simple model system, viz. hard ellipsoids of revolution. The shape of such a spheroid is characterized by a single parameter,  $x$ , the ratio of the length of the major axis ( $2a$ ) to the minor axis ( $2b$ ):  $x = a/b$ . Special cases are:  $x = 1$  (hard spheres),  $x \rightarrow \infty$  (hard needles [13]) and  $x \rightarrow 0$  (hard platelets [17]). Technical details of the Monte Carlo simulations have been published elsewhere [18]. Here I shall concentrate on the results. Nevertheless, in order to facilitate the 'reading' of the figures, I must explain the reduced units in which the results are expressed. All static properties of a (classical) many body

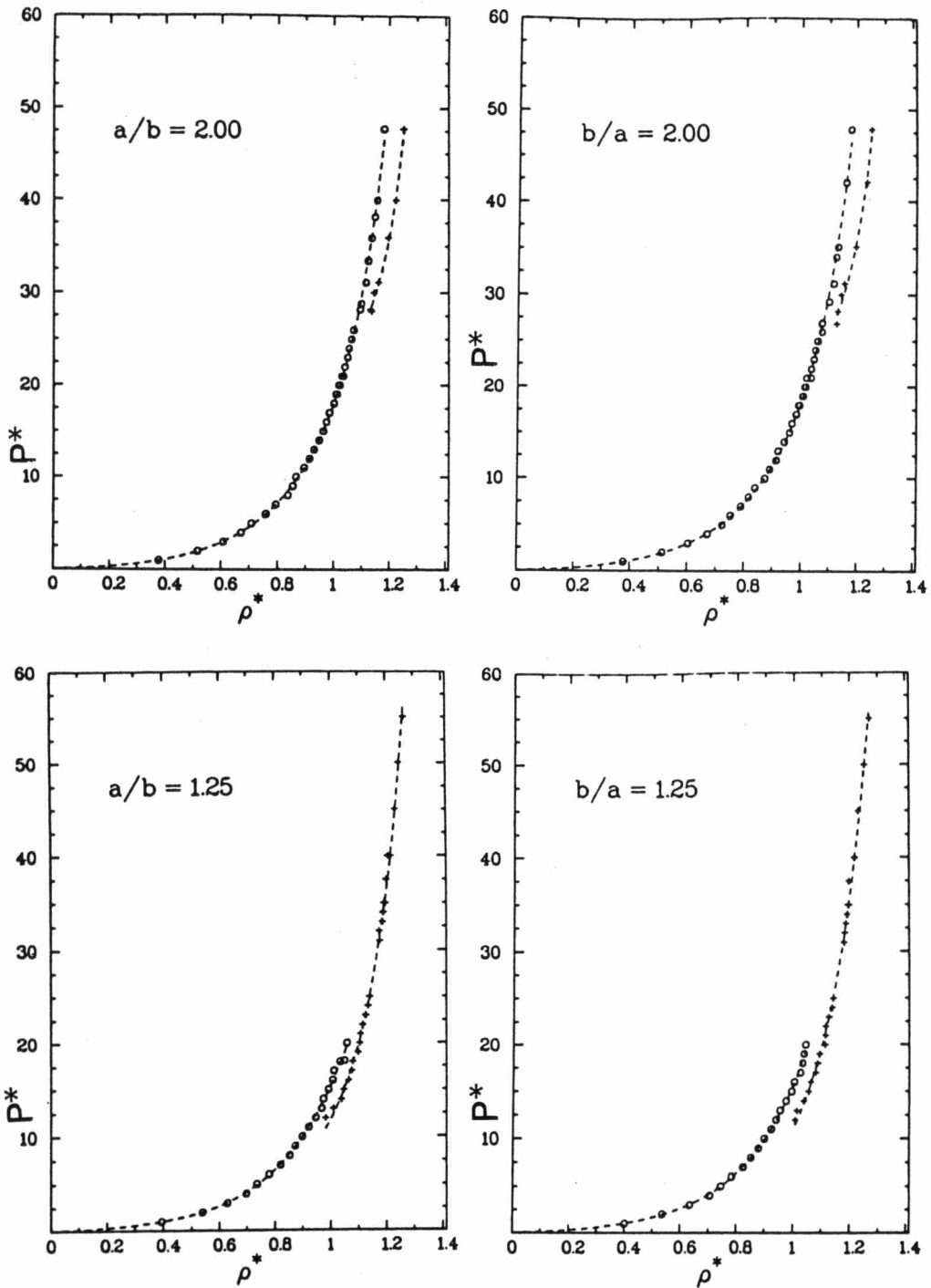


Fig. 1: Equation of state of hard ellipsoids of revolution with length-to-breadth ratios  $x=2, 1.25, 0.8$  and  $0.5$ . The pressure is in units  $kT/8ab^2$ , the density in units  $(8ab^2)^{-1}$ . Open circles: (isotropic) fluid branch, pluses: solid branch.

system can be expressed in units which are derived from two basic units: the unit of length and the unit of energy. For time dependent properties, we need one more fundamental unit: usually, the unit of mass. For a hard-core system, the only 'natural' energy scale is the thermal energy  $kT$ . Hence, we shall express all energies in units  $kT$ . For the unit of length we clearly need a quantity related to the size of the molecules. For ellipsoids it is convenient to use a unit of volume that is proportional to the volume of the particles ( $v_0 = (4\pi/3)ab^2$ ). We use as unit of volume the quantity  $8ab^2$ . The reason for this choice is that it facilitates comparison of the data for spheroids with the known hard-sphere results. For hard spheres, our unit of volume reduces to  $\sigma^3$ , where  $\sigma$  is the hard sphere diameter. One important consequence of this choice of units is that the reduced density of close regular packing for all spheroids equals  $\sqrt{2}$ . The obvious choice for the unit of mass is the mass of one molecule. In addition, the dynamics of non-spherical molecules depend on the moment of inertia. In the example to be discussed below, we have assumed that the mass of the molecules is distributed uniformly over their proper volume.

### III.2 Equation of State

With this background we can consider the Monte Carlo results. We carried out constant pressure Monte Carlo simulations for hard spheroids with 8 different length-to-breadth ratios  $x$  in the range between  $1/3$  (oblate) and  $3$  (prolate). Typical examples of the resulting isotherms are shown in Figure 1. The isotherms shown in Figure 1 consist of two branches: a low density branch corresponding to the isotropic fluid phase, and a high density solid branch. Direct coexistence between solid and liquid cannot be observed in these small systems ( $0(10^2)$  particles) with periodic boundary conditions. In Figure 1 no nematic branch is observed because the molecules are not sufficiently anisometric. What is striking about Figure 1 is the strong resemblance between isotherms for particles with reciprocal length-to-breadth ratios. Actually, we find such almost symmetric behavior for all spheroids that we studied. A more quantitative measure of this symmetry is shown in Figure 2. In this figure the percentual difference of the pressure of oblate and prolate ellipsoids is plotted as a function of density. At low densities this difference goes to zero. This is understandable because, in the present units, the second virial coefficients of spheroids with inverse length-to-breadth ratios are equal [19]. However, no such symmetry holds for the higher virial coefficients. In particular, Onsager has argued that in the limit  $x \rightarrow \infty$ ,  $B_3/B_2^2 \rightarrow 0$ . But in the limit  $x \rightarrow 0$ , this same ratio tends to a finite value of  $0.4447$  [17]. The approximate oblate-prolate symmetry at higher densities shown in Figure 2 is therefore not exact, which makes it all the more surprising.

### III.3 Orientational Order

Let us next look for orientationally ordered phases. Figure 3 shows the equation of states of spheroids with  $a/b > 2.75$  and  $a/b < (1/2.75)$  at densities around the

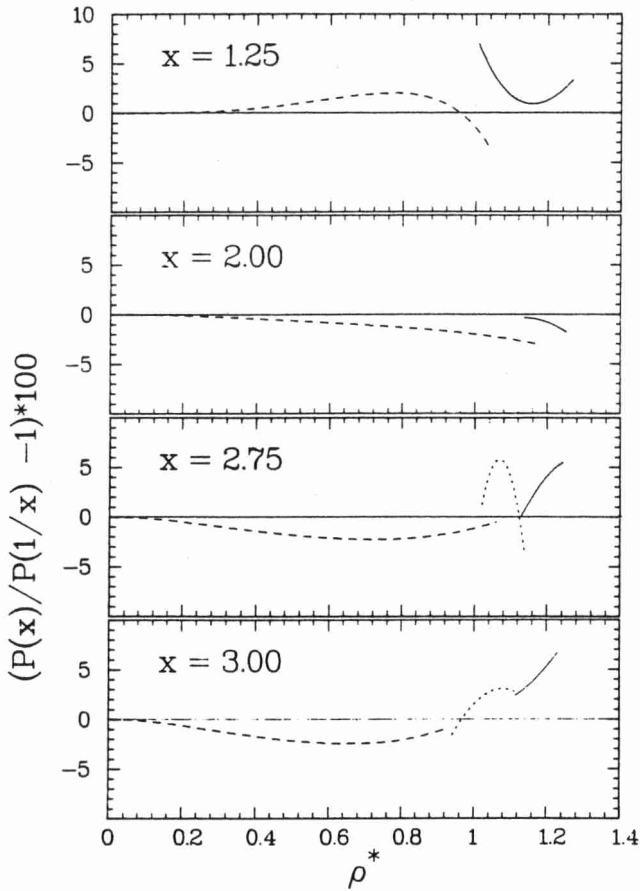


Fig. 2: Deviations from perfect symmetry of the equation of state of hard ellipsoids of revolution with inverse length-to-breadth ratios. The ordinate shows the percentual difference between the pressure of a fluid of hard ellipsoids with  $a/b = x$  and  $b/a = x$ , both at density  $\rho$ . Dashed curve: isotropic branch, dotted curve: nematic branch, drawn curve: solid branch. The curves shown in this figure were obtained from fits to the equation of state data (see Ref. [18]).

melting point. Between the solid and the isotropic fluid branch we observe a third branch which corresponds, as we shall show, to a nematic liquid crystal. There are several methods to detect a nematic phase in a computer simulation. For instance, one may compute the eigenvalues of the collective molecular orientation tensor  $\bar{\bar{Q}}$ :

$$Q_{\alpha\beta} = (1/N \sum \{3u_{\alpha}u_{\beta} - \delta_{\alpha\beta}\})/2. \quad (1)$$

In the isotropic phase, all eigenvalues vanish in the thermodynamic limit. In the nematic phase, the largest eigenvalue equals the nematic order parameter  $S$ . This method, although straightforward in principle, requires some care when applied to finite systems. In particular, the largest eigenvalue of  $\bar{\bar{Q}}$  is always positive. In the isotropic phase it is of order  $1/\sqrt{N}$ , where  $\sqrt{N}$  is the number of particles in the system. This implies that, for instance, in a system consisting of 100 particles, this 'order parameter' is never less than 0.1. Hence it is not a particularly sensitive probe to monitor the onset of orientational order. A less common but more useful measure for the degree of orientational order is -2 times the smallest (in absolute value)

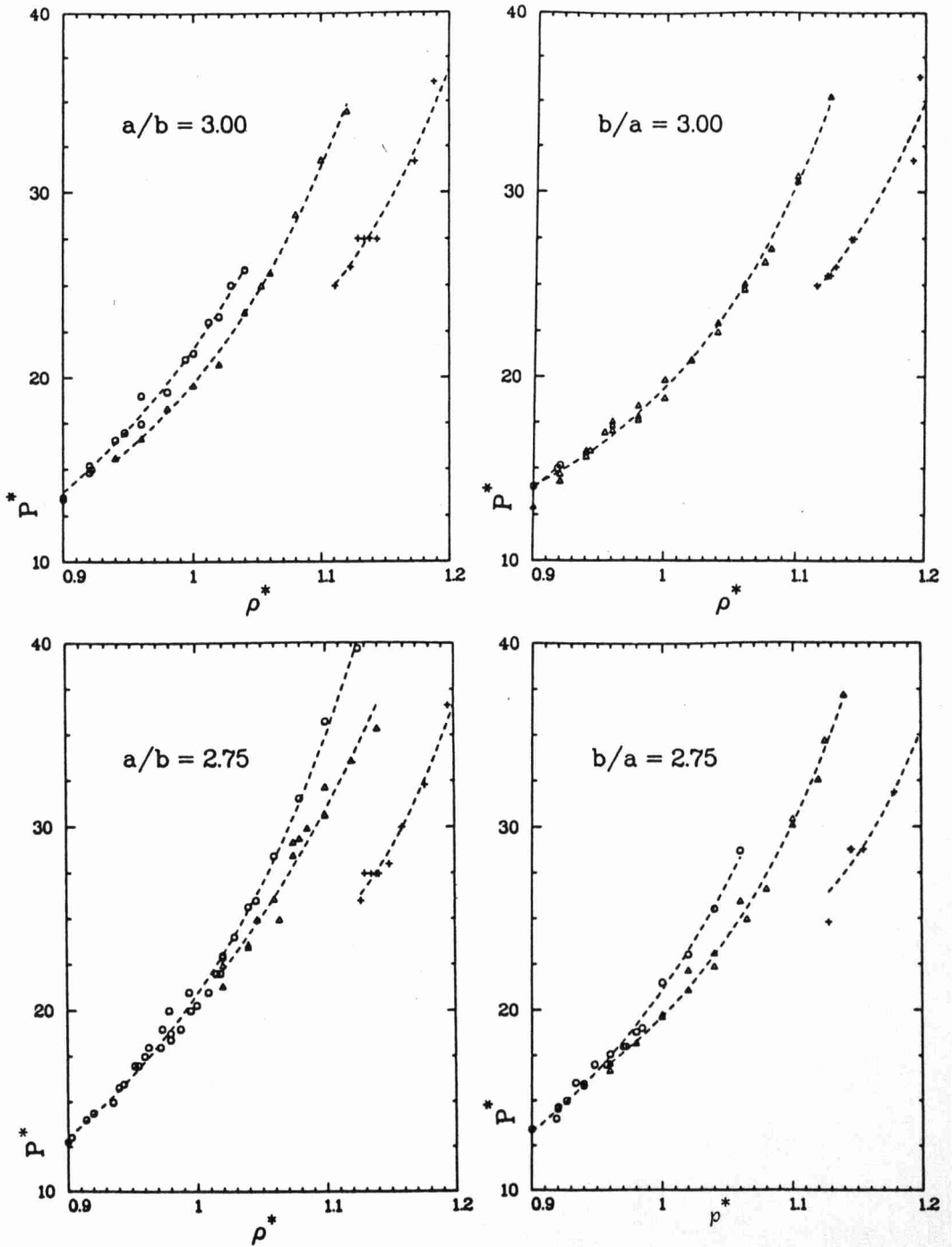


Fig. 3: Equation of state of hard ellipsoids of revolution with length-to-breadth ratios 3, 2.75, 1/2.75 and 1/3, in the density range where a nematic branch is observed. Open circles: (isotropic) fluid branch, triangles: nematic branch, pluses: solid branch. The units are as in Figure 1.

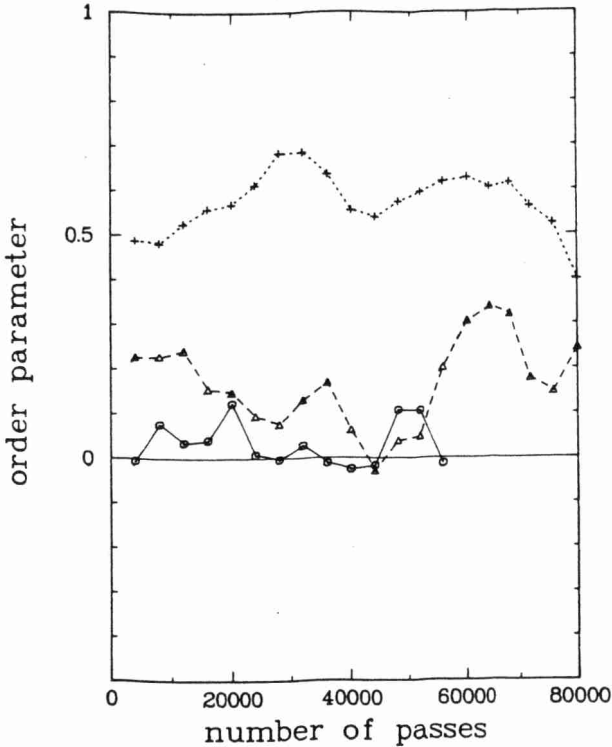


Fig. 4: Slow fluctuations in the nematic order parameter during a Monte Carlo simulation of hard ellipsoids of revolution. Pluses:  $b/a=3$ ,  $\rho/\rho_0=0.69$  (nematic). Open triangles:  $b/a=3$ ,  $\rho/\rho_0=0.65$  (overexpanded nematic). Open squares:  $a/b=3$ ,  $\rho/\rho_0=0.636$  (isotropic). One Monte Carlo pass corresponds to one trial move for every particle.

eigenvalue of  $\bar{Q}$  [17]. This quantity has the desirable property that it is of order  $1/N$  (rather than  $1/\sqrt{N}$ ) in the isotropic phase and, moreover, that it fluctuates around zero. In a (uniaxial) nematic phase, the latter definition of the order parameter is only equivalent to the previous one in the thermodynamic limit. Figure 4 shows that typical fluctuations in this order parameter in the vicinity of the isotropic-nematic transition in a fluid of hard ellipsoids.

An equally simple method to detect the onset of orientational order is to monitor the behavior of the pair distribution function, in particular the part that depends on the relative orientation of molecules at a distance  $r$ . A useful measure of the degree of orientational order is given by  $g_2(r)$ , defined as the average value of  $P_2(\cos\theta)$  for molecules with a center of mass distance  $r$ ;  $\theta$  is the angle between the molecular axes. In the isotropic phase  $g_2(r)$  decays to zero within a few molecular diameters. In contrast, in the nematic phase  $g_2(r)$  becomes long ranged. As  $r \rightarrow \infty$ ,  $g_2(r) \rightarrow S^2$ , where  $S$  is the nematic order parameter. Of course, in a computer simulation we can never measure correlations at distances greater than half the periodic box diameter,  $L$ . But, as Figure 5 shows, even the behaviour of  $g_2$  at  $r = L/2$  is a useful indicator of the onset of orientational order. Figure 5 illustrates another important feature of

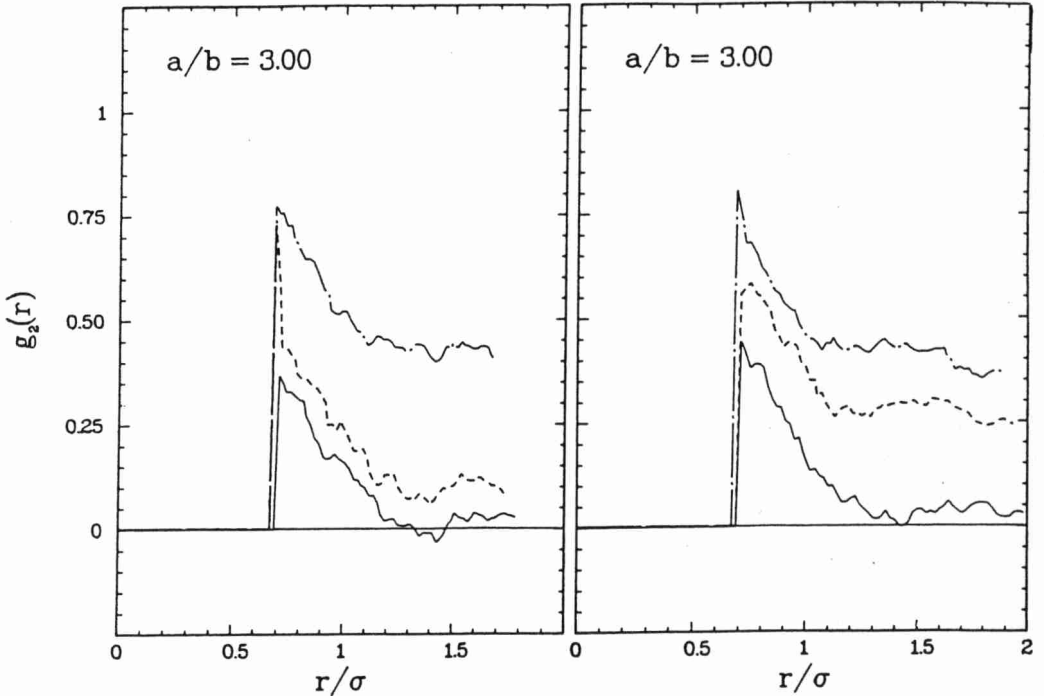


Fig. 5: Example of the behavior of the orientational correlation function  $g_2(r) = \langle P_2(\vec{u}(0) \cdot \vec{u}(r)) \rangle$  of hard ellipsoids of revolution with  $a/b = 3$  in the vicinity of the I-N transition. Densities:  $\rho/\rho_0 = 0.65$  (drawn curve),  $\rho/\rho_0 = 0.707$  (dashed curve), and  $\rho/\rho_0 = 778$  (dash-dot). The left-hand side shows the behavior of  $g_2(r)$  on compression. The right-hand side shows the corresponding results for expansion.

the isotropic-nematic transition in a system of prolate hard ellipsoids, namely the fact that it exhibits hysteresis. Hysteresis is usually observed at first order phase transitions. However, the isotropic-nematic transition is only weakly first order and, as a consequence, hysteresis may be suppressed by fluctuations. For oblate ellipsoids, hysteresis appears to be weaker than for prolate ellipsoids. Why this should be so is not clear at present.

#### III.4 Free Energies and Phase Transitions

In order to map the phase behaviour of the hard ellipsoids as a function of their anisometry, the location of all thermodynamic phase transitions must be determined. Without this information we cannot tell whether the nematic branch in Figure 3 corresponds to a thermodynamically stable phase, and if so, over what range of densities. In computer simulations of other model systems, similar questions arise every time a first order phase transition is observed. It is clearly important to establish whether a new phase is thermodynamically stable or not. Unfortunately, the computational effort involved in locating the coexistence points for first order phase transitions of molecular systems is appreciable. Moreover, the computational techniques that must be used are

not widely known. This warrants a brief 'technical' digression on the numerical location of phase coexistence points.

Let us recall that the condition which must be satisfied at a phase transition is that the temperature  $T$ , the pressure  $P$  and the chemical potential  $\mu$  of the coexisting phases are equal. From the Monte Carlo simulations described above we know the pressure as a function of density for all phases (for hard-core systems the temperature plays no role; we choose  $kT$  as our unit of energy). However, the chemical potential  $\mu$  cannot be derived directly from the equation of state data. The usual method to determine the chemical potential in real experiments is by thermodynamic integration along a reversible path from a reference state of known chemical potential to the state point under consideration. This approach is also applicable to computer simulations. For the isotropic fluid phase the reference state is the ideal gas. Using:

$$P = -(\partial F/\partial V)_T, \quad (2)$$

where  $F$  is the Helmholtz free energy of the system, we can compute  $F$  at a density  $\rho$  by integration:

$$F(\rho, T) = F_{id}(\rho, T) + kT \int_0^\rho d\rho (P/\rho kT - 1)/\rho. \quad (3)$$

For a one-component system,  $\mu$  follows directly from  $F$  because  $\mu = F + PV$ . In principle, the applicability of the thermodynamic integration method sketched above is not limited to the computation of the chemical potential of the isotropic fluid phase. All that is needed is the existence of a reversible path from the ideal gas phase to the phase of interest. In the real world it is perfectly admissible for such a path to cross first order phase transitions, as long as the phase transformation can be carried out reversibly. The problem is that this latter condition is rarely satisfied in computer simulations of first order phase transitions. For the system sizes typically studied by computer simulation, first order phase transitions exhibit strong hysteresis. As a consequence, the transition from one phase to the other usually requires appreciable over-compression/overexpansion and then proceeds irreversibly if at all. Fortunately, in computer simulation one is not restricted to thermodynamic integration along 'natural' paths. Apart from changing the density or temperature one may modify the Hamiltonian  $H$  of the system through application of artificial external fields or through gradual modification of the intermolecular interactions between the particles. The idea is to modify the Hamiltonian in such a way that the resulting model system is sufficiently simple that its free energy can be computed analytically. Let us call this reference free energy  $F_{ref}$ . By gradually changing the Hamiltonian back to its original form, we have constructed a path that joins the phase of interest to a state of known free energy. Of course, such a path is not necessarily reversible. However, by a judicious choice of the parameters that control the variation of the artificial Hamiltonian one can often create reversible paths through 'parameter space'. To give an example, the

free energy of a crystal of hard spheres can be computed by constructing a reversible path from the hard-sphere crystal to an Einstein crystal of the same structure [20]. In this case, the modification of the Hamiltonian is simply that in addition to the intermolecular interactions all atoms are bound to their lattice sites ( $\vec{r}_i^0$ ) by harmonic springs of strength  $\lambda K$

$$H(\lambda) = H_0 + \lambda K \sum_i (\vec{r}_i - \vec{r}_i^0)^2 . \quad (4)$$

For  $\lambda = 0$ , the Hamiltonian corresponds to that of the normal hard-sphere system, while for  $\lambda = 1$  the system behaves as an (almost) ideal Einstein crystal. The derivative of the free energy with respect to  $\lambda$  equals:

$$dF/d\lambda = \langle dH(\lambda)/d\lambda \rangle = K \langle \sum_{i=1}^N (\vec{r}_i - \vec{r}_i^0)^2 \rangle . \quad (5)$$

As the last term on the right hand side of the above equation can be evaluated by Monte Carlo simulation, the free energy difference

$$F(\lambda = 1) - F(\lambda = 0) = \int_0^1 dF/d\lambda \, d\lambda \quad (6)$$

can be computed to any desired degree of accuracy by computing  $\langle \sum_i (\vec{r}_i - \vec{r}_i^0)^2 \rangle$  at a sufficiently large number of intermediate values of the coupling parameter  $\lambda$ .

In order to find the phase transitions for a system of hard ellipsoids, free energy calculations of the type described above must be carried out both for the solid and the nematic phase. In the case of the solid, the reference system is an Einstein crystal with the same structure as the original solid. In this Einstein crystal, harmonic restoring forces reduce the fluctuations of both the translational and the orientational degrees of freedom around their equilibrium values. The situation is slightly more complex for the nematic phase, because in this case the reference state clearly cannot be a crystal. One possible approach is described in Ref. [18]. The reference state is an ideal gas in a strong aligning field. The nematic phase is reached in two stages. First the aligned gas is compressed to a density at which the system without field is in a nematic phase, and then the aligning field is slowly switched off. This approach makes use of the fact that the first-order isotropic-nematic transition is suppressed in a sufficiently strong field, in much the same way that the liquid-vapour transition is suppressed along a supercritical isotherm. For this reason the path from the reference state (the dilute gas in a field) to the nematic phase, is free of phase transitions.

### III.5 Phase Diagram

Using the methods described above, the free energy of all phases of the system of hard ellipsoids was computed and the phase transitions located. The resulting 'phase diagram' is shown in Figure 6. In this figure the molecular shape is varied from left to right from extremely oblate ellipsoids ('platelets'), through spheres to extremely prolate

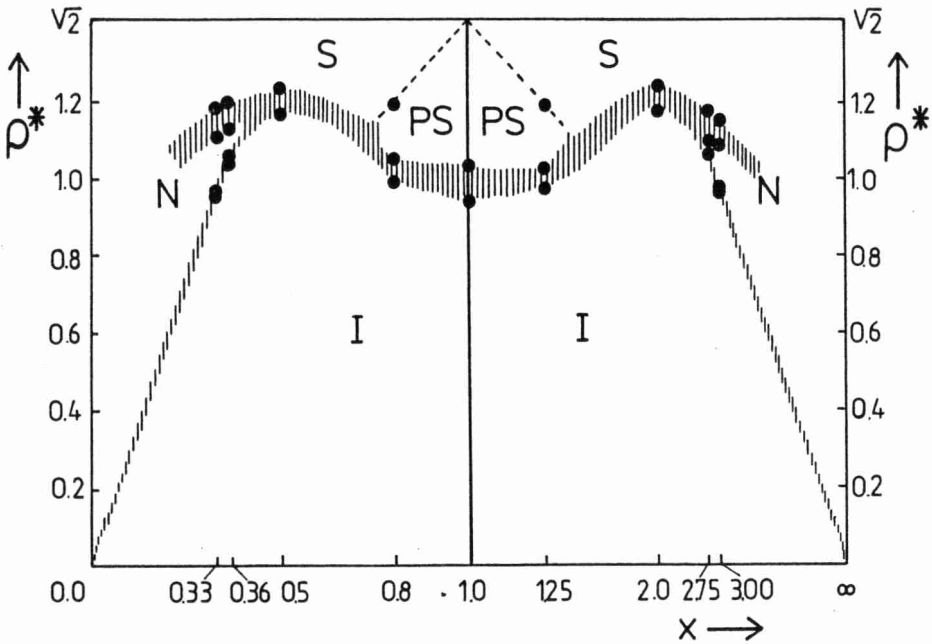


Fig. 6: 'Phase diagram' of hard ellipsoids of revolution. Vertical axis: density in units  $(8ab^2)^{-1}$ . Horizontal axis: Length-to-breadth ratio,  $x$ . The shaded areas correspond to two-phase regions. The dots are the computed coexistence points. The points for  $x=1$  were taken from Ref. [16]. The following phases can be distinguished: isotropic fluid (I), nematic liquid crystal (N), orientationally ordered solid (S) and plastic solid (PS).

ellipsoids ('needles'). The ordinate measures the density which, in the present units, varies between 0 and  $\sqrt{2}$  (regular close packing). Four distinct phases can be identified, the isotropic fluid (I), nematic fluid (N), orientationally ordered solid (S) and orientationally disordered (plastic) solid (PS). The shaded areas represent two-phase coexistence regions. Several aspects of Figure 6 are worth noting. First of all the overall phase diagram has a high degree of symmetry under the interchange of oblate and prolate ellipsoids. As in Figure 2 above, this symmetry is not perfect. Still, the physical reason for this near symmetry is not understood at present. Figure 6 also provides us with an answer to the old question: what is the minimum non-sphericity needed to form a stable nematic phase? Clearly, for ellipsoids with axial ratios approximately between  $1/2.5$  and  $2.5$ , no stable nematic phase is possible. As a bonus, we obtain an estimate of the range of stability of the orientationally disordered solid phase (approximately between  $a/b = 1/1.5$  and  $a/b = 1.5$ ) although in this case the boundaries are less well-determined.

Now that we know the range of stability of the nematic phase in this model system, let us look in more detail at the physical consequences of the onset of orientational ordering. In the isotropic phase, the presence of a nematic is betrayed by an increase in the amplitude of collective orientational fluctuations. Below we shall illustrate what computer simulation can tell us about such pretransitional phenomena.

### III.6 Orientational Precursor Effects

At the transition to the nematic phase spontaneous ordering of the molecular orientations takes place. Although this macroscopic ordering occurs at a well-defined state point, strong pretransitional fluctuations may be observed in the isotropic phase as the transition to the nematic phase is approached. Actually, the fact that such pretransitional fluctuations can be observed at all is due to the peculiar nature of the isotropic-nematic transition. After all, this is a first-order phase transition, and usually there are no precursor effects near such phase transitions (such as, for instance, the freezing transition). The isotropic-nematic transition is different because it is a 'weak' first-order transition; it exhibits most of the 'critical' pretransitional behaviour typical for a continuous phase transition, but before the 'critical' point is reached, a first-order transition intervenes. The classical language to describe pretransitional fluctuations in the vicinity of an (almost)-second-order phase transition was developed by Landau [21]. The basic assumption in the Landau theory of phase transitions is that the free energy density  $F$  can be written as a power series in the order parameter  $S$ :

$$F(S) = F_0 + AS^2 + BS^3 + CS^4 + \dots, \quad (7)$$

where  $A, B, C$ , etc. are coefficients that depend on temperature and/or density. For a second-order phase transition ( $B=0$ ), the coefficient  $A$  changes sign at the transition density  $\rho^*$ . In the vicinity of the transition  $A$  is assumed to be a linear function of  $(\rho^* - \rho)$ :

$$A(\rho) = a(\rho^* - \rho). \quad (8)$$

For a weakly first-order phase transition ( $B \neq 0$ ),  $A$  still goes to zero, at a density  $\rho^*$  which is, however, slightly higher than the actual transition point  $\rho_{IN}$ . The most likely value of the order parameter is found by minimizing  $F(S)$  with respect to  $S$ . Depending on the values of  $A, B$  and  $C$  this minimum may be situated at  $S = 0$  (isotropic phase) or at  $S > 0$  (nematic phase). For  $B^2 = 4AC$ ,  $F(S)$  has two equivalent minima, one at  $S = 0$ , the other at  $S = -B/2A$ . This is the point where isotropic and nematic phases are in equilibrium. In a Monte Carlo simulation it is possible to 'measure'  $F(S)$  directly, because  $P(S)$ , the probability density for observing a particular value of the order parameter  $S$  is proportional to  $\exp(-\beta F(S))$ .  $P(S)$  is obtained by collecting a histogram of the fluctuations in  $S$  during a Monte Carlo run.  $F(S)$  then follows from  $\beta F(S) = \text{constant} - \ln(P(S))$ . Figure 7 shows an example of the behaviour of  $F(S)$  as the isotropic-nematic transition is crossed. Note that information about large values of  $F(S)$  resides in the wings of  $P(S)$  where the statistics tend to be poor. As a consequence, only the lowest few coefficients of the Landau-de-Gennes expansion can be determined by Monte Carlo simulation. In order for the Landau expansion to be useful as a phenomenological description, the coefficients  $B$  and  $C$  should be

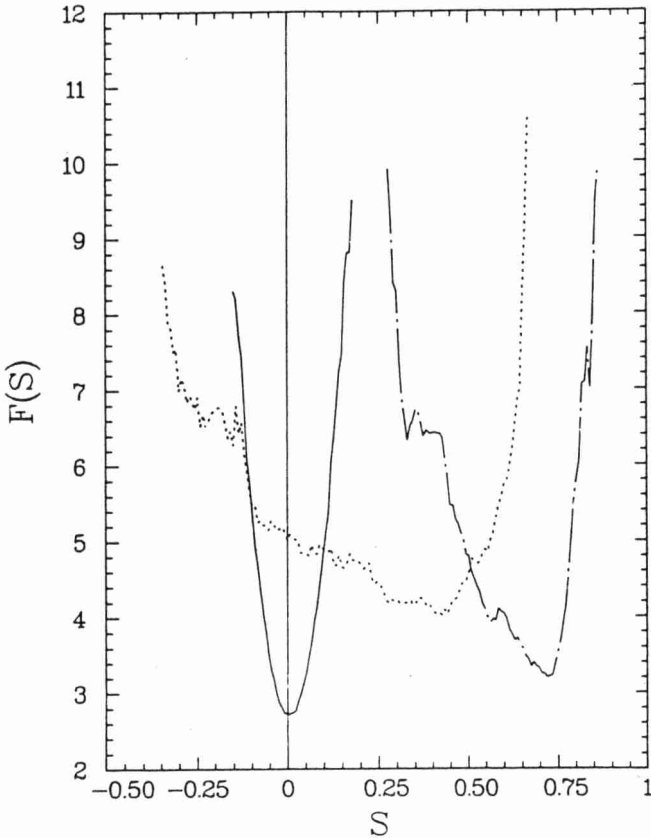
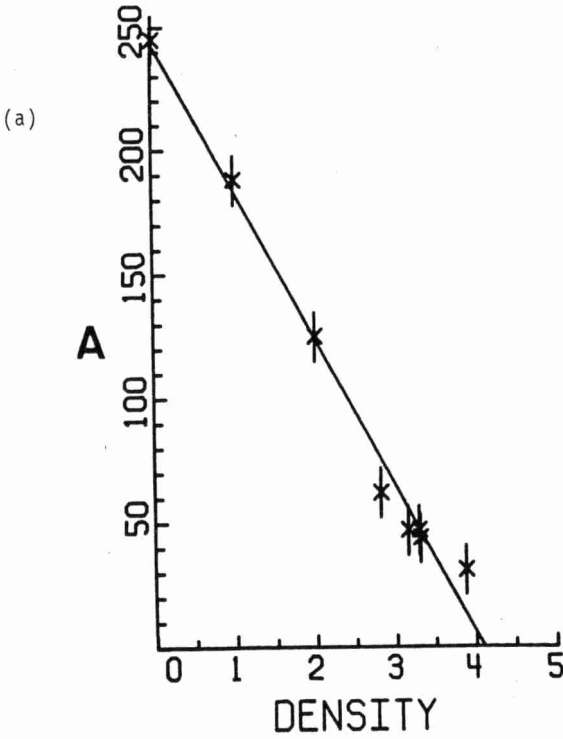
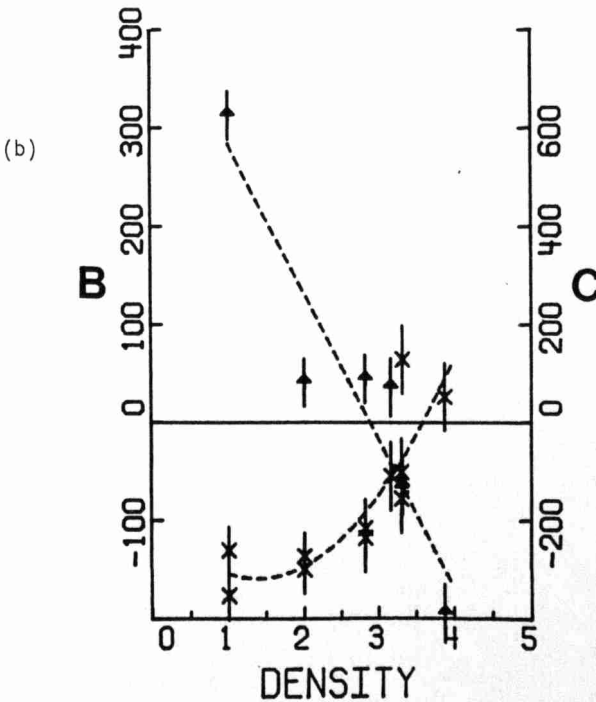


Fig. 7: The Landau free energy  $F(S)$  (in units  $kT$ ) associated with fluctuations of the nematic order parameter  $S$  in a system of 100 hard platelets of diameter  $\sigma$  (see Ref. [17]). Drawn curve: low density isotropic phase. Dotted curve: higher density, just beyond the isotropic-nematic transition. Note that the minimum of  $F(S)$  is shifting to a non-zero value of  $S$ . Dash-dot curve: high density nematic. Now only small fluctuations around a non-zero average value of  $S$  are possible.

slowly varying functions of  $\rho$ , while  $A$  should change sign close to the thermodynamic transition point. Figure 8 shows that  $A$  does indeed behave more or less as predicted by Eq. (8). The statistical errors in  $B$  (and even more in  $C$ ), are large. Yet the data shown in Figure 8 seem to suggest that  $B$  (and possibly  $C$ ) is in fact changing appreciably in the vicinity of the isotropic-nematic transition. This unexpected behaviour of the Landau coefficients was also observed in a simulation of a very different model system [22]. The numerical results suggest that the Landau-de-Gennes theory may not correctly describe the non-Gaussian order-parameter fluctuations in the vicinity of the isotropic-nematic transition. However, more detailed calculations are needed to clarify this point. For a discussion of the Landau-de-Gennes theory in the context of recent experiments on real nematogens, the reader is referred to a review by Gramsbergen, Longa and de Jeu [23]. This review also discusses experimental evidence for non-Gaussian order-parameter fluctuations in the vicinity of the isotropic-nematic transition.



**Fig. 8:** Density dependence of the coefficients of the lowest few powers of  $S$  in the Landau expansion:  $F(S) = \text{constant} + AS^2 + BS^3 + CS^4 + \text{higher order terms}$ . The model is a system of 100 infinitely thin hard platelets (see Ref. [17]). Note that  $A$  ((a)) extrapolates to zero at the I-N transition.  $B(x)$  appears to change sign in the vicinity of the I-N transition. The statistical error in  $C(\blacktriangle)$  is very large.



Although interesting from a fundamental point of view, non-Gaussian effects play a relatively minor role in the pretransitional behaviour of nematogens. The most striking effect that is observed as the isotropic-nematic transition is approached from the isotropic side is the strong increase in the amplitude of order-parameter fluctuations, which results, among other things, in enhanced depolarized light scattering. To a first approximation, the intensity of depolarized light scattering,  $I_d$ , is proportional to the average trace of the square of the collective orientational tensor  $\overline{Q}$  defined in Eq. (1) above:

$$I_d \sim \langle Q_{\alpha\beta} Q_{\beta\alpha} \rangle = 3/2 \langle S^2 \rangle. \quad (9)$$

From the Landau-de-Gennes expansion (7) and the relation between  $P(S)$  and  $F(S)$  it follows that, in the Gaussian approximation,  $\langle S^2 \rangle \sim A^{-1}$  and hence:

$$I_d \sim (\rho^* - \rho)^{-1}. \quad (10)$$

$\langle Q_{\alpha\beta} Q_{\beta\alpha} \rangle$  in Eq. (9) is a measure for the correlation of the orientation of different molecules. Using Eqs. (1) and (9), it is easy to show that  $\langle S^2 \rangle = (1 + g_2)/N$ , where  $g_2$  is the static orientational correlation factor, defined as:

$$g_2 = \frac{\sum_{j \neq i} P_2(\vec{u}_i \cdot \vec{u}_j)}{N}. \quad (11)$$

The proximity of the isotropic-nematic transition influences not just the static orientational properties of the fluid but also the rotational dynamics. In particular, the relaxation time  $\tau_2^C$  of the collective orientational fluctuations diverges as the I-N transition is approached. The relation between the divergence of  $g_2$  and  $\tau_2^C$  is of particular interest. Using Mori theory, Keyes and Kivelson [24] derived the following expression relating  $g_2$  to  $\tau_2^C$  [25]:

$$\tau_2^S / \tau_2^C = (1 + j_2) / (1 + g_2). \quad (12)$$

Here  $\tau_2^S$  is the single-particle correlation time and  $j_2$  is the dynamic orientational correlation factor. The latter quantity can be expressed in terms of memory functions, but has no simple physical interpretation. A direct experimental determination of  $(1 + g_2)$  and  $\tau_2^S / \tau_2^C$  is complicated by the fact that in real liquids part of the depolarized light scattering intensity is interaction induced. It is not trivial to separate out the purely orientational contribution to the scattering intensity [26]. As a consequence, there is a scarcity of reliable data from which  $j_2$  can be determined. The available information (see e.g. [27]) suggests that  $j_2$  is small compared to 1, and it is common practice among light scatterers to assume that  $j_2 = 0$ .

Numerical simulation offers a unique possibility to study the static and dynamic precursor effects to the I-N transition in simple model systems. As an example, we

consider the pretransitional behaviour in a system of prolate and hard ellipsoids with  $a/b=3$  [28]. From the Monte Carlo simulations mentioned above, we know that this system has a transition from the isotropic to the nematic phase at 70% of the density of regular close packing [18]. For comparison, we also studied the orientational dynamics of hard ellipsoids with  $a/b=2$ . The latter system has no stable nematic phase and hence we should expect it to behave rather differently from the more anisometric  $a/b=3$  system. Figure 9 shows typical examples of  $C_1^S(t) \equiv \langle P_1(\vec{u}(0) \cdot \vec{u}(t)) \rangle$  and  $C_2^S(t) \equiv \langle P_2(\vec{u}(0) \cdot \vec{u}(t)) \rangle$ , the correlation functions of the first and second Legendre polynomials of the molecular orientation vectors. Both  $C_1^S(t)$  and  $C_2^S(t)$  are single-particle correlation functions [19]. In the rotational diffusion limit, the ratio of the relaxation times of  $C_1^S(t)$  and  $C_2^S(t)$ ,  $\tau_1^S/\tau_2^S$  equals 3. We find that this behavior well obeyed at not too low densities. Both single particle relaxation times grow as the density is

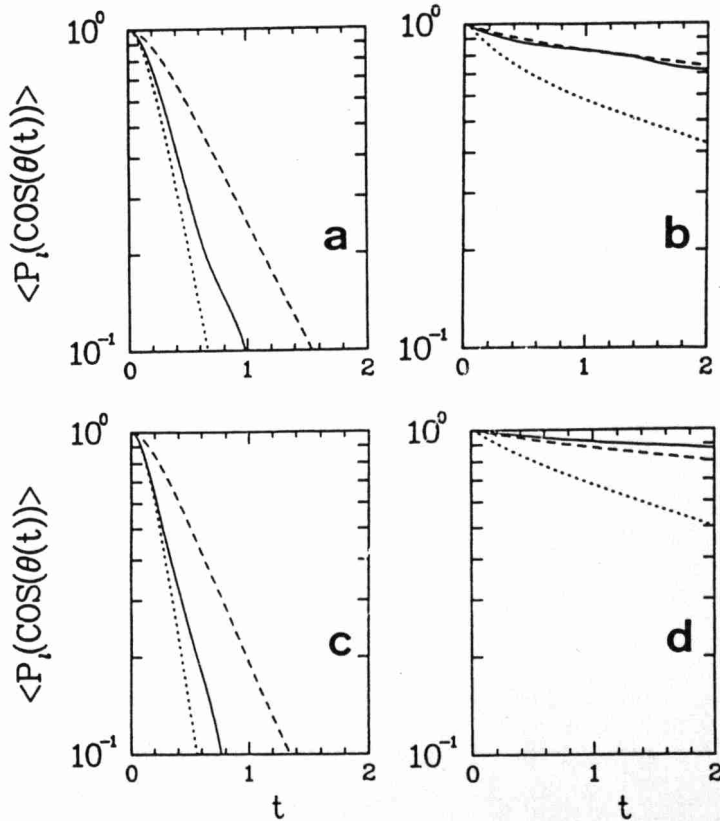


Fig. 9: Density and shape dependence of single-particle and collective orientational correlation function for hard ellipsoids of revolution. Figure A:  $a/b = 2$ ,  $\rho/\rho_0 = 0.5$ , figure B:  $a/b = 2$ ,  $\rho/\rho_0 = 0.8$ , figure C:  $a/b = 3$ ,  $\rho/\rho_0 = 0.3$  and figure D:  $a/b = 3$ ,  $\rho/\rho_0 = 0.7$ . (---) Single-particle first-rank orientational correlation function,  $C_1^S(t) = \langle P_1(\vec{u}(0) \cdot \vec{u}(t)) \rangle$ . (···) Single-particle second-rank orientational correlation function,  $C_2^S(t) = \langle P_2(\vec{u}(0) \cdot \vec{u}(t)) \rangle$ . (—) Collective second-rank orientational correlation function,  $C_2^C(t) = \sum_j \langle P_2(u_1(0) \cdot u_j(t)) \rangle$ . The single-particle orientational variable has been made orthogonal to the collective one by projection. Note that at high densities the decay of  $C_2^C(t)$  becomes much slower than that of  $C_2^S(t)$ .

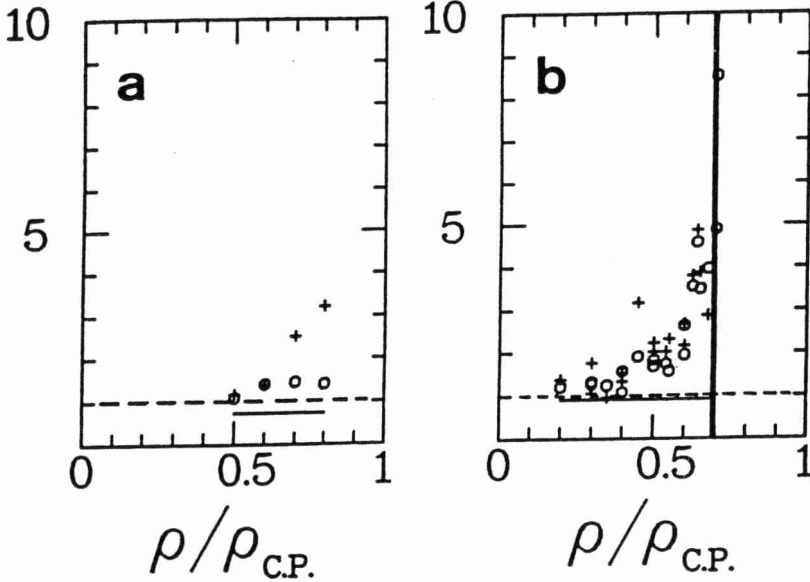


Fig. 10: Density dependence of the ratio  $\tau_2^C/\tau_2^S$  (pluses), for hard ellipsoids of revolution with  $a/b=2$  (figure A) and  $a/b=3$  (figure B). Also shown is the behavior of the static orientational correlation factor  $(1+g_2)$  (open circles). The best estimate for the dynamic orientational correlation factor  $(1+j_2)$  is shown as a horizontal line. In figure B the isotropic-nematic coexistence region is bordered by parallel vertical lines.

increased. This is simply a consequence of the rapid increase of the viscosity as the density of the fluid is raised, and the effect is observed for both shapes of ellipsoids. The density dependence of the collective orientational correlation function,  $C_2^C(t) \equiv \langle \sum_j \langle P_2(\vec{u}_1(0) \cdot \vec{u}_j(t)) \rangle \rangle$  is more interesting. At low densities, the decay of  $C_2^C(t)$  closely follows that of  $C_2^S(t)$ , as can be seen from Figure 9. However, as the density is increased, the decay of the collective orientational correlation function becomes much slower than the corresponding single particle one. Hence, cooperative effects in the rotational dynamics become important at high densities, both for the  $a/b=2$  and for  $a/b=3$  case. Figure 10 shows the density dependence of the ratio  $\tau_2^C/\tau_2^S$  for both shapes of ellipsoids. In the same figure we have also plotted the corresponding values of  $(1+g_2)$ . The difference in the behaviour of the  $a/b=3$  and  $a/b=2$  ellipsoids is immediately apparent. For  $a/b=2$  there is evidence for some cooperative behaviour, but even at the freezing density (at 84% of close packing), there is no sign of diverging fluctuations or critical slowing down. In contrast, the results for  $a/b=3$  clearly show pretransitional effects. Both  $\tau_2^C/\tau_2^S$  and  $(1+g_2)$  appear to diverge as the transition to the nematic phase is approached. If the dynamic orientational correlation factor  $j_2$  vanishes, then the data points for  $\tau_2^C/\tau_2^S$  and  $(1+g_2)$  should superimpose. On this point the simulations appear inconclusive. The statistics on  $\tau_2^C/\tau_2^S$  and  $(1+g_2)$  are poor, even though these are fairly long runs ( $0(10^6)$  collision for a 144 particle system). The reason for the large scatter in the data points is that the

quantities shown are collective properties. The signal-to-noise ratio for such quantities is of order  $\sqrt{(\tau/T)}$ , where  $\tau$  is a characteristic relaxation time, and  $T$  is the duration of the simulation [30]. Hence, as the correlation times of the collective orientational fluctuations grow larger, the statistics (for a fixed value of  $T$ ) become worse. Clearly, it is not meaningful to extract estimates for  $j_2$  from the individual data points. We therefore attempted to estimate  $j_2$  in the following way. We assumed  $(\tau_2^S / \tau_2^C)(1+g_2) (=1+j_2)$  was independent of density, and carried out a linear least squares fit to the data points. The results of these fits are indicated as drawn lines in Figure 10. We see that for both shapes the estimate for  $(1+j_2)$  is less than 1. For the  $a/b=3$  case, where we have the largest number of data points, the fit suggests that  $j_2$  is small and negative (typically  $-0.08 \pm -0.05$ ). For the  $a/b=2$  ellipsoids the estimated value of  $j_2$  is slightly larger ( $-0.26 \pm -0.16$ ), but the estimated error is larger. It is amusing to note that a  $j_2$  of the same sign and comparable magnitude followed from the light-scattering experiments of Gierke and Flygare on a real nematogen ( $j_2 = -0.3 \pm -0.3$  for MBBA) [27]. We do not wish to attach too much significance to the actual numbers that we have obtained for  $j_2$ : clearly, much longer simulations are needed to carry out a direct comparison with the relevant theoretical predictions. In fact, such simulations are now in progress. The importance of the preliminary results presented here is that they provide the first numerical data on pretransitional effects in the orientational dynamics of any model nematogen. In addition, our results indicate that the numerical determination of  $j_2$ , although time-consuming, is certainly feasible.

#### IV. Beyond Nematics

##### IV.1 Introduction

In the previous sections we have shown that sufficiently anisometric hard ellipsoids of revolution can form thermodynamically stable nematic phases. And that, moreover, these simple model systems exhibit many of the static and dynamic properties of real nematogens. Naturally, the question arises whether the nematic phase is the only type of liquid crystal that can be simulated with a hard-core model. For instance, one might wonder whether hard ellipsoids of revolution can also form a smectic phase, i.e. a fluid that has (at least) one-dimensional translational order, in addition to the orientational order already present in nematics (see e.g. Ref. [8]). The answer to this question is almost certainly: no. The reason is the following: smectic phases tend to have a large degree of orientational order (i.e. the order parameter  $S$ , defined in Section III.3 above, is close to 1). Hence, to a first approximation, we can assume that a smectic consists of perfectly aligned, non-spherical molecules. However, a system consisting of hard ellipsoids of revolution with axial ratio  $a/b$ , all parallel to the  $z$ -axis (say), can be mapped onto the hard-sphere fluid by a simple scaling of all  $z$ -coordinates with a factor  $b/a$ . As hard spheres apparently do not form smectics, parallel hard ellipsoids cannot do so either. So, unless the orientational degrees of

freedom stabilize the smectic phase (and this seems unlikely), hard ellipsoids of revolution cannot form smectics.

The question then arises whether smectic phases can be formed by other rigid hard-core models. This is not obvious a priori. In fact, to my knowledge, most textbooks on liquid crystals do not even seriously consider the possibility (see, however, Ref. [31]). Even more than in the case of nematics, dispersion forces [32] and the effects of flexible tails [12] are held responsible for the formation of smectic phases. Although we do not contest that these factors must have a pronounced effect on the stability of smectics, the question that must be answered is whether they are essential in the same way that attractive forces are essential to explain the liquid-vapour transition [33].

## IV.2 Computer Simulations

In order to explore the possibility of smectic order in rigid hard-core systems, we carried out Monte Carlo and Molecular Dynamics simulations on model systems consisting of parallel spherocylinders with diameter  $D$  and length  $L$  (i.e. the hemispherical caps were separated by a straight cylindrical segment of length  $L$ ) [34]. As the particles in this system are always perfectly aligned, the low-density phase is a "nematic" fluid. The parallel spherocylinder fluid can be thought of as a model for a fluid of rodlike particles in a strong magnetic field. As mentioned above, we know that the corresponding hard-ellipsoid model will not exhibit smectic order. Simulations were carried out for systems of parallel spherocylinders with  $L/D$  ratios of 0.25, 0.5, 1, 2, 3 and 5. The well-known case  $L/D=0$  (i.e. hard spheres) was also studied, as a check. System sizes varying from 90 to 1080 particles were studied. Initially, the system was prepared in a regular close-packed lattice. We prepared this lattice by expanding a close-packed face-centered cubic hard-sphere crystal by a factor  $(L/D+1)$  along the [111]-axis. In order to avoid spurious translational order due to incomplete melting, the crystals were expanded to low densities (typically, 30% of close-packing), where the solid rapidly melted to form a translationally disordered fluid. Fluid configurations at higher densities were subsequently generated by slow compression. In contrast, solid configurations were generated by gradual expansion from the close-packed lattice. During the simulations of the solid phase we allowed for changes in the shape of the crystal unit cell, using an isotropic-stress Monte Carlo method, as described in Ref. [18]. In addition, we computed the absolute free energies of both the fluid and the solid phases, employing the techniques described in Section III.4 and Ref. [34]. Combining the free energy and equation of state data, we can determine the dependence of the melting point of the spherocylinder crystal on  $L/D$  (see Table I). Having determined the limits of thermodynamic stability of the solid phase, the next step is to look for possible fluid-fluid phase transitions. No discontinuities or van der Waals loops are observed in the fluid branch of the equation of state [34], but for the larger  $L/D$  ratios we observe a rather sudden change in the compressibility at densities

**Table I:** Densities and pressures of the solid-liquid coexistence points of parallel spherocylinders with length-to-width ratios  $L/D$  between 0.25 and 5.0.

$L/D$	$\rho/\rho_0$ (fluid)	$\rho/\rho_0$ (solid)	$P_{FS}$
0.25	0.610	0.685	4.75
0.50	0.612	0.665	4.58
1.00	0.624	0.650	4.50
2.00	0.751	0.802	9.99
3.00	0.771	0.818	11.22
5.00	0.693	0.759	7.83

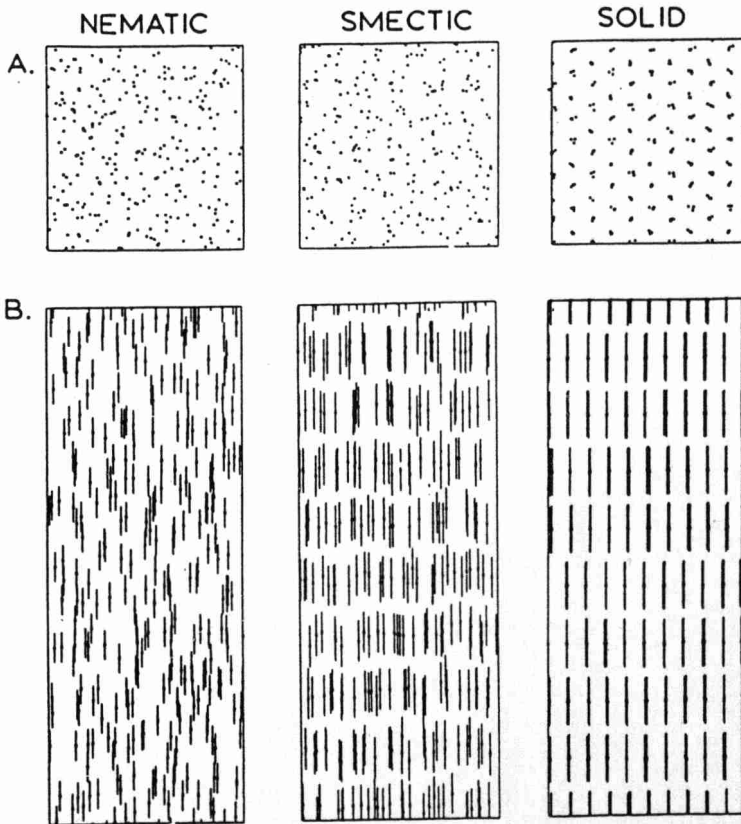


**Fig. 11:** Snapshots of typical configurations of a system of 270 parallel hard spherocylinders with  $L/D=5$ . Left: nematic phase ( $\rho/\rho_0=0.24$ ). Middle: smectic phase ( $\rho/\rho_0=0.62$ ). Right: solid phase ( $\rho/\rho_0=0.89$ ). The upper figures (A) show a projection in the plane perpendicular to the molecular axes, the lower figures (B) show a projection in a plane through the molecular axes. For the sake of clarity, the spherocylinders are indicated by a line segment of length  $L$ .

between 40% and 60% of close packing. Snapshots of typical molecular configurations both below and above this 'cusp' in the equation of state (Figure 11) show a dramatic change in the structure of the fluid. At low densities, the fluid is translationally disordered. Then, at a higher density (but well before the freezing point), the fluid orders into parallel layers, but there is no order within the layers. In other words, the parallel spherocylinders form a smectic A-phase [35]. For comparison, the crystalline phase, at still a higher density, is also shown. In the latter case there is clearly translational order within the layers.

A more quantitative method to locate the transition to the smectic phase is to study the static and dynamic behaviour of the longitudinal component of the intermediate scattering function  $F(k_z, t)$ , defined as:

$$F(k_z, t) = \langle \rho(k_z, 0) \rho(-k_z, t) \rangle, \quad (15)$$

where  $\rho(k_z, t)$  is the instantaneous amplitude of a longitudinal density fluctuation with wavevector  $k_z$ .  $F(k_z, t=0)$  is the longitudinal part of the static structure factor,  $S(k_z)$ , which determines, for instance, the x-ray scattering intensity. As the smectic phase is approached from lower densities, there will be smectic precursor fluctuations. These will show up as peaks in  $S(k_z)$ , for values  $k_z$  equal to (multiples of)  $2\pi/d$ , where  $d$  is the spacing of the incipient smectic layers. If the transition to the smectic phase is continuous, the peaks in  $S(k_z)$  will diverge at the transition. An example of this behaviour is shown in Figure 12. If we define the smectic layer

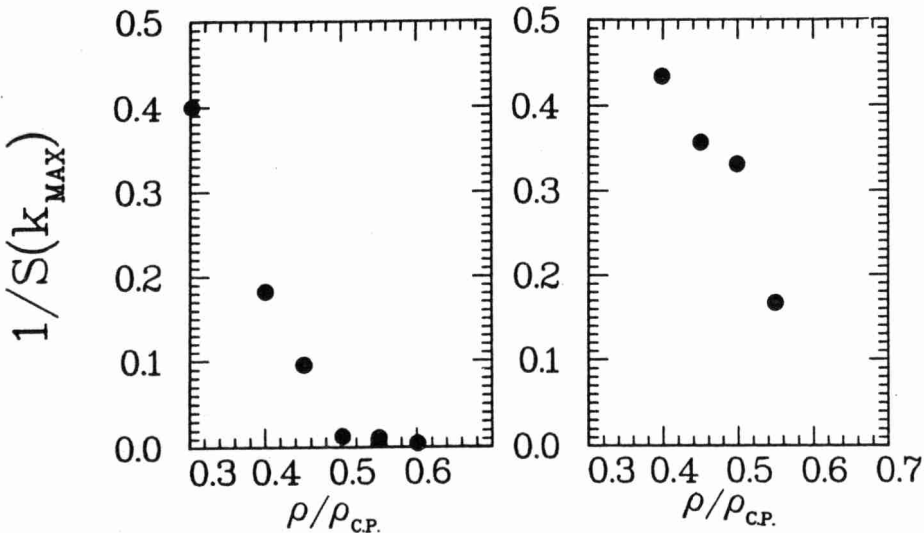


Fig. 12: Density dependence of the first maximum in the longitudinal component of the structure factor of parallel hard spherocylinders with  $L/D=5$  (left) and  $L/D=0.5$  (right). The ordinate shows  $1/S(k_{\text{MAX}})$ . In the dilute gas, this quantity approaches one. In a smectic phase it should vanish in the thermodynamic limit. The present results apply to a 270-particle system, hence  $1/S(k_{\text{MAX}}) \geq 1/270$ . From the behaviour of  $S(k_{\text{MAX}})$  one may deduce the density dependence of the longitudinal correlation length of  $\xi_{\parallel}$  of smectic precursor fluctuations.

spacing  $d$ , by  $d = 2\pi/k_z(\text{max})$ , where  $k_z(\text{max})$  is the wavevector corresponding to the first (and largest) maximum in  $S(k_z)$ , then we can measure how many smectic layers fit into the simulation box. Figure 13 shows how the number of layers depends on density

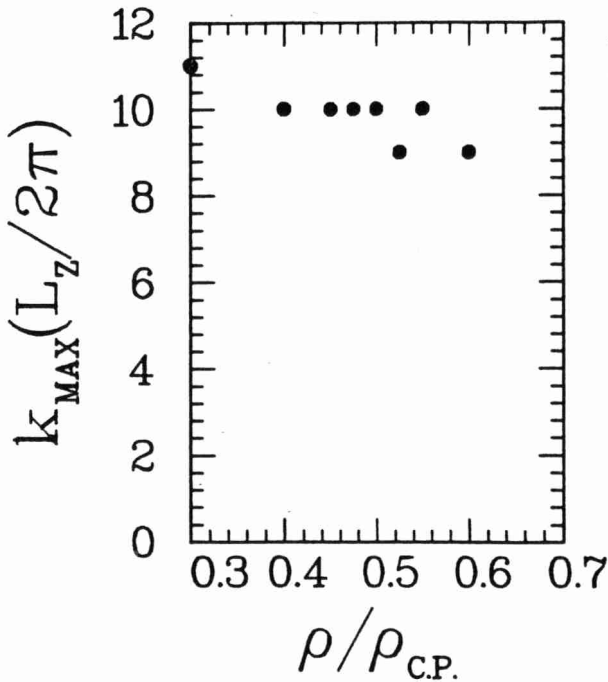


Fig. 13: Density dependence of the 'number of layers' in a system of 270 parallel spherocylinders with  $L/D=5$ . The number of layers is defined as the number of oscillations of the largest longitudinal Fourier component in the periodic box:  $k_{max}L_z/2\pi$ . Note that the observed layering is not a metastability effect associated with the insufficient equilibration of the initial configuration.

for  $L/D = 5$ . The fact that the number of layers is not constant but changes on compression, is gratifying. It indicates that the number of layers is an equilibrium property, and not the consequence of some residual, metastable solid order (the solid phase, in this case, consists of 9 layers). The ordering of the fluid in layers has a pronounced effect on the diffusion of individual particles. At low densities, the longitudinal component of the self-diffusion,  $D_\ell$ , constant is larger than the transverse component,  $D_t$ . This effect is strongest for the most elongated particles. But as smectic layers start to form at higher densities, the  $D_\ell$  decreases much more rapidly than  $D_t$ . So much so, that in the smectic phase  $D_t$  becomes larger than  $D_\ell$  (see Figure 14). Hence, in the smectic phase, intra-layer diffusion is more rapid than inter-layer diffusion. Incidentally, this effect is also observed in some real liquid crystals [36].

A particularly sensitive probe of incipient smectic ordering is the critical slowing down of the correlation function  $\langle \rho(k_z, 0)\rho(-k_z, t) \rangle$  at  $k_z = k_z(\text{max})$ . As can be seen from Figure 15, the decay rate of  $F(k_z(\text{max}), t)$  first increases as the density is raised, because the fluid is less compressible at higher densities. But beyond a certain density the decay rate drops precipitously to zero. This provides us with an estimate for the nematic-smectic transition density. For comparison, Figure 15 also shows an example of a fluid which does not become smectic ( $L/D=0.25$ ). In this case the decay rate of  $F(k_z(\text{max}), t)$  depends only weakly on density.

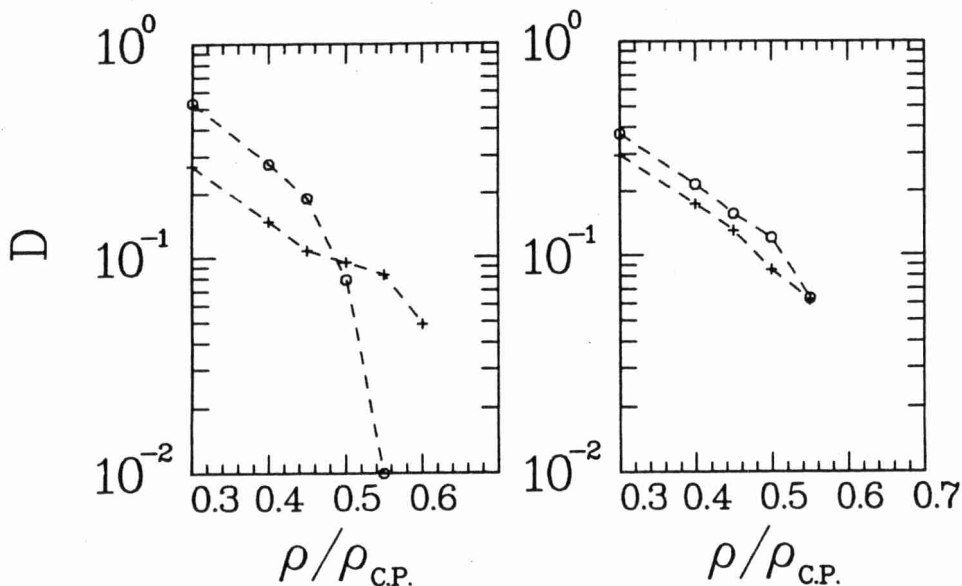


Fig. 14: Typical example of the density dependence of the longitudinal (O) and transverse (+) components of the self-diffusion tensor in a system of parallel spherocylinders with  $L/D=1$  (left) and  $L/D=0.25$  (right). Note that the relative magnitudes of the parallel and perpendicular components of  $D$  change as the fluid goes from the nematic to the smectic phase.

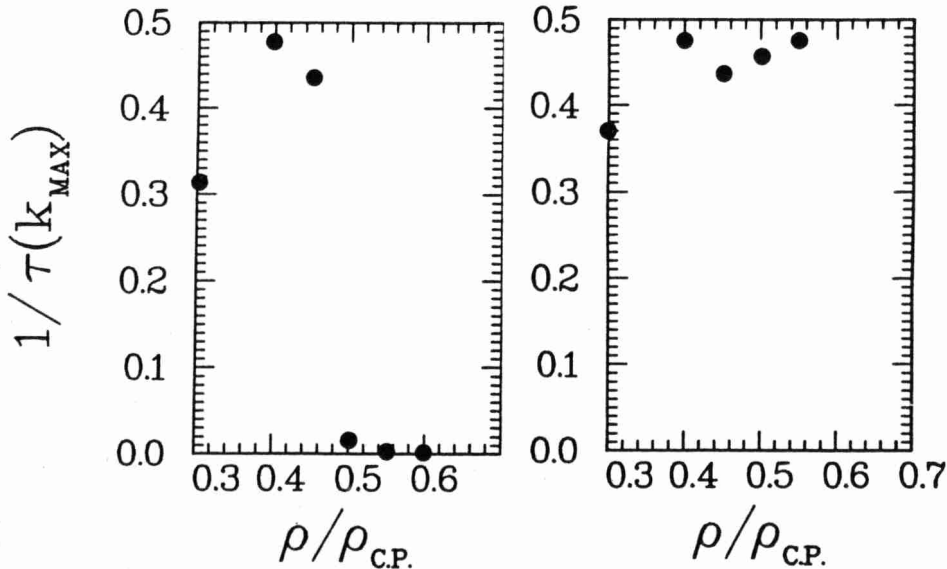


Fig. 15: Relaxation rate of the longitudinal density fluctuations with a wavevector corresponding to the first maximum in  $S(k_2)$ . Right figure: parallel spherocylinders with  $L/D = 0.25$ , this system does not form a stable smectic. The figure shows no evidence for critical slowing down. Left hand figure: parallel spherocylinders with  $L/D = 1$ . This system does form a smectic. As the transition is approached, the decay rate of the smectic precursor fluctuations drops dramatically.

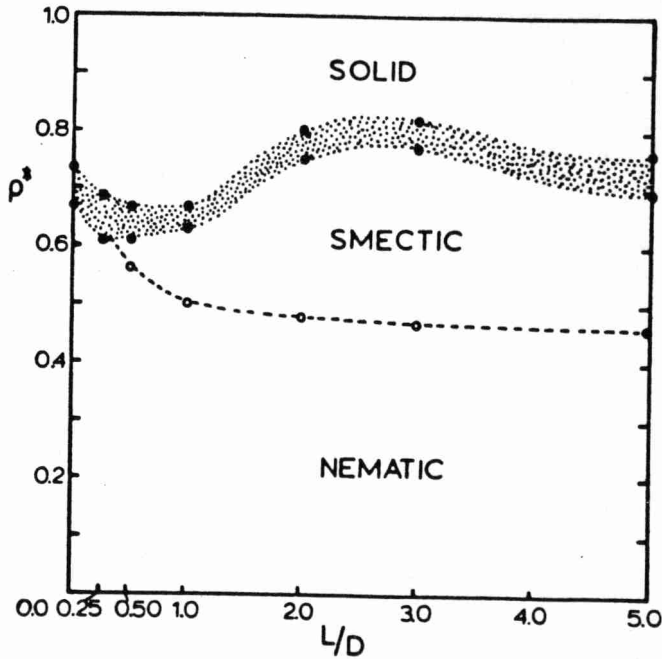


Fig. 16: Schematic 'phase diagram' of hard parallel spherocylinders, as a function of length-to-width ratio  $L/D$ . The shaded area corresponds to the fluid-solid two-phase region. Black circles: densities of the coexisting fluid and solid phase. Open circles: densities at which smectic ordering sets in. The dashed line indicates the estimated nematic-smectic boundary.

Combining the information about the smectic order parameter fluctuations with the data in Table I on the melting transition, we can construct a 'phase diagram' of hard parallel spherocylinders (Figure 16). This phase diagram shows the regions of stability of the nematic, smectic and solid phases as a function of  $L/D$ . For  $L/D \geq 0.5$ , a smectic phase is found between the crystalline solid and the 'nematic' fluid. As the non-sphericity of the particles is increased, the smectic range initially grows and then saturates [37]. It should be stressed that this phase diagram pertains to a system of parallel spherocylinders. The effect of the orientational degrees of freedom on the phase diagram is currently under investigation [38].

## V. Conclusions

In this paper I have tried to demonstrate that model systems consisting of non-spherical hard-core particles have a surprisingly rich phase diagram. In the case of hard ellipsoids, we found that the stability of the nematic phase is simply related to the degree of non-sphericity of the molecules. Moreover, even though parallel ellipsoidal particles cannot form stable smectics, parallel spherocylinders can. This result is quite unexpected because of the apparent similarity of long spherocylinders and needle-like ellipsoids.

In addition I have shown how many of the physically interesting static and dynamic properties of liquid-crystal-forming fluids can be studied by computer simulation. The interest of such calculations lies not in the possibility to reproduce the behaviour of real liquid crystals (although it is encouraging to find qualitative agreement). The use of these, and future, calculations is that they can be used to test approximate theoretical expressions for a wide variety of equilibrium and transport properties of molecular liquids and liquid crystals. Moreover, now that we have demonstrated the existence of stable hard core nematics and (aligned) smectics for 'realistic' molecular shapes, we can prepare for the next step: thermodynamic perturbation theory.

There is more to liquid crystals than hard repulsive interactions. In the next few years we should be able to decide whether hard-core models are useful reference systems for real liquid crystals.

#### Acknowledgements

The material presented in this article is the result of collaboration with: Mike Allen, Rob Eppenga, Henk Lekkerkerker, Bela Mulder and Alain Stroobants. The work of the FOM Institute for Atomic and Molecular Physics is part of the research program of FOM and is supported by the "Nederlandse Organisatie voor Zuiver Wetenschappelijk Onderzoek."

#### References

- [1] J.D. van der Waals, Dissertation, Leiden 1873. For a discussion of the van der Waals model in the context of the modern theory of liquids, see: B.J. Alder and W.G. Hoover, in: *The Physics of Simple Liquids*, H.N.V. Temperley, J.S. Rowlinson and G.S. Rushbrooke, eds., North Holland, Amsterdam 1968, p. 79
- [2] J.A. Barker and D. Henderson, *J. Chem. Phys.* **48**, 4714 (1967)
- [3] J.D. Weeks, D. Chandler and H.C. Andersen, *J. Chem. Phys.* **54**, 5237 (1971)
- [4] H.S. Kang, T. Ree and F.H. Ree, *J. Chem. Phys.* **84**, 4547 (1986)
- [5] B.J. Alder and T.E. Wainwright, *J. Chem. Phys.* **27**, 1208 (1957)
- [6] See, for instance, C. Zannoni in: *The molecular physics of liquid crystals*. G.R. Luckhurst and G.W. Gray, editors, Academic Press, London, 1979, p. 51
- [7] S.J. Picken, Internal report, University of Groningen (1984)
- [8] P.G. de Gennes, *Physics of Liquid Crystals*, Oxford University Press, 1974
- [9] W. Maier and A. Saupe, *Z. Naturf.* **A13**, 564 (1958)
- [10] W.M. Gelbart and A. Gelbart, *Mol. Phys.* **33**, 1387 (1977)
- [11] This holds for thermotropic liquid crystals. For lyotropic liquid crystals flexible tails play no role, although here the flexibility of the particle as a whole may be important, see: T. Odijk, *Polymer Comm.* **26**, 197 (1985)
- [12] F. Dowell and D.E. Martire, *J. Chem. Phys.* **68**, 1088 (1978), *ibid.*: **68**, 1094 (1978), *ibid.*: **69**, 2322 (1978)  
F. Dowell, *Phys. Rev.* **A28**, 3526 (1983)
- [13] L. Onsager, *Ann. N.Y. Acad. Sci.* **51**, 627 (1949)
- [14] See e.g. G.W. Gray in: *The molecular physics of liquid crystals*. G.R. Luckhurst and G.W. Gray, editors, Academic Press, London, 1979, pp. 1 and 263

- [15] C. Destrade, P. Fouchet, H. Gasparoux, N.H. Tinh, A.M. Levelut and J. Malthee, *Mol. Cryst. Liq. Cryst.* 106, 121 (1984)
- [16] W.G. Hoover and F.H. Ree, *J. Chem. Phys.* 49, 3609 (1968)
- [17] R. Eppenga and D. Frenkel, *Mol. Phys.* 52, 1303 (1984)
- [19] A. Isihara, *J. Chem. Phys.* 19, 1142 (1956)
- [20] D. Frenkel and A.J.C. Ladd, *J. Chem. Phys.* 81, 3188 (1984)
- [21] L.D. Landau, *Phys. Z. Sowjetunion* 11, 26 (1937)  
For a discussion of Landau theory in the context of the isotropic-nematic transition see: P.G. de Gennes, Ref. [8]
- [22] G.R. Luckhurst, personal communication
- [23] E.F. Gramsbergen, L. Longa and W.H. de Jeu, *Physics Reports* 135, 197 (1986)
- [24] T. Keyes and D. Kivelson, *J. Chem. Phys.* 56, 1057 (1974)
- [25] Unfortunately, there is some confusion in the literature about the notation used for the static and dynamic correlation factors ( $1+g_2$ ) and ( $1+j_2$ ). Here we have chosen a definition of  $g_2$  and  $j_2$  such that both quantities vanish in the absence of correlations.
- [26] For a discussion, see: D. Kivelson and P.A. Madden, *Ann. Rev. Phys. Chem.* 31, 523 (1980)
- [27] G.R. Alms, T.D. Gierke and W.H. Flygare, *J. Chem. Phys.* 61, 4083 (1974)  
T.D. Gierke and W.H. Flygare, *J. Chem. Phys.* 61, 2231 (1974)
- [28] M.P. Allen and D. Frenkel, *Phys. Rev. Lett.* 58, 1748 (1987)
- [29] Actually, the correlation functions shown are the orthogonalized single-particle and collective orientational correlation functions.
- [30] R. Zwanzig and N.K. Ailawadi, *Phys. Rev.* 182, 280 (1969)
- [31] M. Hosino, H. Nakano and H. Kimura, *J. Phys. Soc. Japan* 46, 1709 (1979)
- [32] W.L. McMillan, *Phys. Rev.* A4, 1238 (1971)
- [33] Actually, transitions from a dilute to a condensed fluid phase need not always be caused by attractive interactions. The crucial point is that hard-core repulsion alone cannot explain such phase transitions.
- [34] A. Stroobants, H.N.W. Lekkerkerker and D. Frenkel, *Phys. Rev. Lett.* 57, 1452 (1986)
- [35] We also checked for long-range bond-orientational order within the layers, but did not find any. Hence the fluid is not a hexatic-B phase.
- [36] M. Hara, H. Tenmei, S. Ichikawa, H. Takezoe and A. Fukuda, *Jap. J. Appl. Phys.* 24, L777 (1985)
- [37] More recent evidence indicates that the phase diagram is even richer than shown in the figure. A. Stroobants, H.N.W. Lekkerkerker and D. Frenkel, submitted for publication
- [38] D. Frenkel, *J. Phys. Chem.*, in press